 FDMP, vol.15, no.2, pp.107-123, 2019

Mixed Convection of Bingham Fluid in a Two Sided Lid-Driven Cavity Heated From Below

Toufik Benmalek[1], Ferhat Souidi[1], Mourad Moderres[2, *], Bilal Yassad[1] and Said Abboudi[3]

Abstract: This study aims to analyze mixed convection in a square cavity with two moving vertical walls by finite volume method. The cavity filled with Non-Newtonian fluid of Bingham model is heated from below and cooled by the other walls. This study has been conducted for certain parameters of Reynolds number (Re=1-100), Richardson number (Ri=1-20), Prandtl number (Pr=1-500), and Bingham number has been studied from 0 to 10. The results indicate that the increase in yield stress drops the heat transfer and the flow become flatter, while increasing Reynolds number augments it. The convective transport is dominant when increasing Richardson number which leads to enhance heat transfer in the cavity for both Newtonian and Non-Newtonian fluid. A correlation of Nusselt number is given in function of different parameters.

Keywords: Mixed convection, heat transfer, Bingham fluid, lid-driven cavity.

1 Introduction

Mixed convection, such as in a lid driven cavity, occurs in many fields in nature and in wide engineering applications such as cooling of electronic devices, food processing, crystal growth, solar power collector, drying technologies.

Many investigations on fluid flow and heat transfer in cavities with moving walls have been conducted by various authors [Kuhlmann, Wanschura and Rath (1997); Khanafer and Chamkha (1999); Kuhlmann, Albensoeder and Blohm (2001); Albensoeder and Kuhlmann (2002); Blohm and Kuhlmann (2002); Cheng and Hung (2006); Mahapatra, Nanda and Sarkar (2006); Shah, Rovagnati, Mashayek et al. (2007); Al-Amiri, Khanafer, Bull et al. (2007); Khanafer, Al-Amiri and Pop (2007); Sharif (2007)]. Furthermore, Oztop et al. [Oztop and Dagtekin (2004)] have analyzed mixed convection in a two sided lid driven cavity for three different configurations. They have found that heat transfer is higher for low Richardson numbers, and is important in the case of aiding forces compared to the other

[1] Laboratoire de mécanique des fluides théorique et appliqué, USTHB, B.P.32, El-Alia, Bab-Ezzouar, 16111 Alger, Algérie.

[2] Laboratory of Industrial Fluids, Measurements and Applications (FIMA), UDBKM, 44225, Ain Defla, Algeria.

[3] Laboratoire M3MUTBM, 90010 Belfort Cedex, France.

[*] Corresponding Author: Mourad Moderres. Email: mouradw002@gmail.com.

configuration. Ouertatani et al. [Ouertatani, Cheikh, Beya et al. (2009)] have simulated three dimensional mixed convection in a double lid driven cubical cavity at various Reynolds and Richardson numbers. The fluid flow and heat transfer induced by the combined effects of the driven lid and the buoyancy force within rectangular enclosures have been investigated by Waheed [Waheed (2009)]. He studied various parameters such as the Prandtl number, Richardson number and aspect ratio at a fixed Reynolds number, Re=100. Sivakumar et al. [Sivakumar, Sivasankaran, Prakash et al. (2010)] have performed analysis of the mixed convection heat transfer in lid-driven cavities with different heating portion lengths at different locations. Cheng [Cheng (2011)] has studied the flow and heat transfer in two-dimensional square cavity where the flow is induced by a shear force resulting from the motion of the upper lid combined with buoyancy force due to bottom heating.

More recently, Muthtamilselvan et al. [Muthtamilselvan and Doh (2014)] have studied heat enhancement of nanofluid in a lid-driven cavity with uniform and non-uniform heating of the bottom wall. Abu-Nada et al. [Abu-Nada and Chamkha (2014)] have analyzed mixed convection flow of a nanofluid in a lid-driven cavity with a wavy wall. Mixed convection of a copper-water nanofluid in a shallow inclined lid driven cavity using the lattice Boltzmann method has been investigated by Karimipour et al. [Karimipour, Esfe, Safaei et al. (2014)]. The study of combined effect of Reynolds and Grashof numbers on mixed convection in a lid-driven T-shaped cavity filled with water-Al_2O_3 nanofluid has been done by Mojumder et al. [Mojumder, Saha, Saha et al. (2015)].

The present study aims to investigate mixed convection in a lid-driven cavity filled with a non-Newtonian fluid based on the Bingham model. These kinds of fluids named viscoplastic materials, exhibit a so-called ''yield stress''. For low stress levels, it behaves like a solid and like a fluid when exceeding this yield stress. Many typical viscoplastic fluids exist, such as pastes, gels, foams, drilling fluids, food and pharmaceutical products.

Many authors have focused on the natural convection of Bingham fluid for different geometries. Zhang et al. [Zhang, Vola and Frigaard (2006)] have studied the effects of yield stress on Rayleigh-Benard convection. Other investigations on this field have been conducted by Turan et al. [Turan, Chakraborty and Poole (2010,2012); Turan, Sachdeva, Poole et al. (2011); Turan, Poole and Chakraborty (2012)]. They have analyzed the effects of Bingham, Rayleigh and Prandtl numbers on fluid flow and heat transfer. Recently, the effects of aspect ratio on natural convection of Bingham fluid in rectangular cavity heated from below were analyzed by Yigit et al. [Yigit, Poole and Chakraborty (2015)] for different Rayleigh and Bingham numbers. They found that heat transfer decreases with an increase of Bingham number and aspect ratio. Mixed convection in a Bingham plastic fluid from a heated hemi-sphere has been investigated numerically in the so-called aiding buoyancy configuration by Nalluri et al. [Nalluri, Patel and Chhabra (2015)], for different Reynolds, Prandtl, Richardson and Bingham numbers.

2 Problem description and mathematical formulation

The geometry of the present investigation is given by Fig. 1. It consists of a two dimensional square cavity of length L. The bottom wall is maintained at high temperature T_H whereas the others at a lower temperature T_C. The vertical walls are moving down, i.e., against gravity, while the horizontal walls are fixed. The cavity is filled with a non-

Newtonian Bingham fluid, and the flow is assumed to be incompressible, laminar and steady. Furthermore, it is considered that density varies according to Boussinesq approximation and the viscous dissipation in the energy equation is neglected.

The strain rate dependence of viscous stresses for yield stress fluids obeying the Bingham model can be expressed as following:

$$\begin{cases} \dot{\gamma} = 0 & \tau \le \tau_0 \\ \tau = \tau_0 + \mu_p \dot{\gamma} & \tau > \tau_0 \end{cases}$$

To avoid the discontinuity on the shear stress, we used the regularized constitutive equation proposed by Papanastasiou [Papanastasiou (1987)] given by:

$$\eta_{app} = 1 + \frac{Bn}{\dot{\gamma}}\left(1 - \exp(-m\dot{\gamma})\right) \tag{1}$$

where "η_{app}" is the apparent viscosity of fluid, and 'm' is a constant presents the stress growth exponent which have the dimension of time, and it depends on μ_p andτ_0. This version of Bingham model has been used by Mahapatra et al. [Mahapatra, Nanda and Sarkar (2006); Zhang, Vola and Frigaard (2006); Shah, Rovagnati, Mashayek et al. (2007)].

With the assumptions mentioned above, and by introducing the non-dimensional variables:

$$x = \frac{x'}{L}\ , y = \frac{y'}{L}\ , u = \frac{u'}{V}\ ,\ v = \frac{v'}{V}\ ,$$

$$p = \frac{p'}{\rho V^2}\ , \mu = \frac{\mu'}{\mu_P}\ , \theta = \frac{T - T_C}{T_H - T_C}$$

The dimensionless form of the governing equations is then:

$$\frac{\partial u}{\partial x} + \frac{\partial u}{\partial y} = 0 \tag{2}$$

$$u\frac{\partial u}{\partial x} + v\frac{\partial u}{\partial y} = -\frac{\partial p}{\partial x} + \frac{1}{Re}\frac{\partial}{\partial x}\left(2\eta_{app}\frac{\partial u}{\partial x}\right) + \frac{1}{Re}\frac{\partial}{\partial y}\left(\eta_{app}\left(\frac{\partial u}{\partial y} + \frac{\partial v}{\partial x}\right)\right) \tag{3}$$

$$u\frac{\partial v}{\partial x} + v\frac{\partial v}{\partial y} = -\frac{\partial p}{\partial y} + \frac{1}{Re}\frac{\partial}{\partial x}\left(\eta_{app}\left(\frac{\partial u}{\partial y} + \frac{\partial v}{\partial x}\right)\right) + \frac{1}{Re}\frac{\partial}{\partial y}\left(2\eta_{app}\frac{\partial v}{\partial y}\right) + Ri\theta \tag{4}$$

$$u\frac{\partial \theta}{\partial x} + v\frac{\partial \theta}{\partial y} = \frac{1}{RePr}\left(\frac{\partial^2\theta}{\partial x^2} + \frac{\partial^2\theta}{\partial y^2}\right) \tag{5}$$

With the boundary conditions:

$x = 0, \quad 0 < y < 1, \quad u = 0, \quad v = -1, \quad \theta = 0$
$x = 1, \quad 0 < y < 1, \quad u = 0, \quad v = -1, \quad \theta = 0$
$y = 0, \quad 0 < x < 1, \quad u = 0, \quad v = 0, \quad \theta = 1$
$y = 1, \quad 0 < x < 1, \quad u = 0, \quad v = 0, \quad \theta = 0$

The dimensionless parameters that govern the fluid flow and heat transfer are:

Bingham number: $B_n = \frac{\tau_0\ L}{V\ \mu_p}$

Grashof number: $Gr = \frac{g\beta L^3 (T_H - T_C)}{\vartheta^2}$

Prandtl number: $Pr = \frac{C\mu_p}{k}$

Reynolds number: $\mathrm{Re} = \frac{\rho V L}{\mu_P}$

Richardson number: $\mathrm{Ri} = \frac{\mathrm{Gr}}{\mathrm{Re}^2}$

The Nusselt number is given by:

$$\mathrm{Nu_x} = \frac{h\,L}{K} = -\left.\frac{\partial\theta}{\partial y}\right|_{y=0} \tag{6}$$

The average Nusselt number along the heated wall is calculated by:

$$\mathrm{Nu} = \int_0^1 \mathrm{Nu_x}\,dx \tag{7}$$

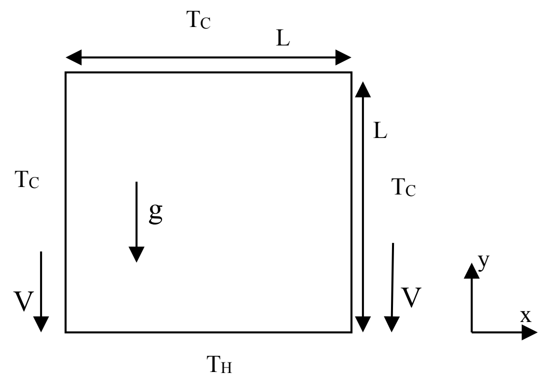

Figure 1: Geometry of the present study

3 Solution of the problem

In the current study, the dimensionless governing equations with boundary conditions are discretized using finite-volume method [Patankar (1980)]. The algorithm SIMPLER is used for the velocity-pressure coupling with under-relaxation technique using power-law scheme. An iterative process is utilized to get the dynamic and the thermal fields, while the convergence criterion is set to 10^{-6} as given by:

$$\left|\frac{\varnothing_{n+1}(i,j) - \varnothing_n(i,j)}{\varnothing_{n+1}(i,j)}\right| \leq 10^{-6}$$

We confirm that reducing these convergence criteria had a negligible effect on the results.

3.1 Grid independency test

To obtain a grid independency, an analysis of grid sensitivity is performed for the mixed convection in the cavity. Five grids were tested as shown in Tab. 1 which depicts the correspondent average Nusselt numbers. Tab. 1 shows clearly that the difference between the results of the average Nusselt number obtained for the 61×61 and the 81×81 grid size is negligible. For this reason, the grid of 61×61 nodes is adopted for all computations reported in this study.

Table 1: Different grids used to test mesh dependence

Mesh	21*21	41*41	61*61	81*81	101*101
Nu (R_i=10)	2.8573	2.8602	2.8612	2.8614	2.8615
Nu (R_i=1)	4.0756	4.8487	4.8597	4.8597	4.8597
Nu (R_i=0.1)	4.8597	8.7861	8.7861	8.7861	8.8706

3.2 Code validation

To validate our approach, the code has been checked against two previous investigations, the first one is a comparison of the velocity distributions with the results of Oztop et al. [Oztop and Dagtekin (2004)] given by Fig. 2(a), and the second one is a comparison of the pressure distributions with the results of Mitsoulis et al. [Mitsoulis and Zisis (2001)] given by Fig. 2(b). The two comparisons show very good agreement.

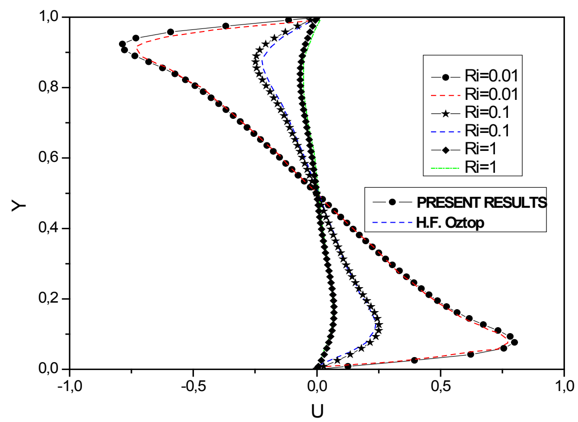

Figure 2: (a) Comparison of velocity profiles at the vertical centerline for different R_i numbers numbers

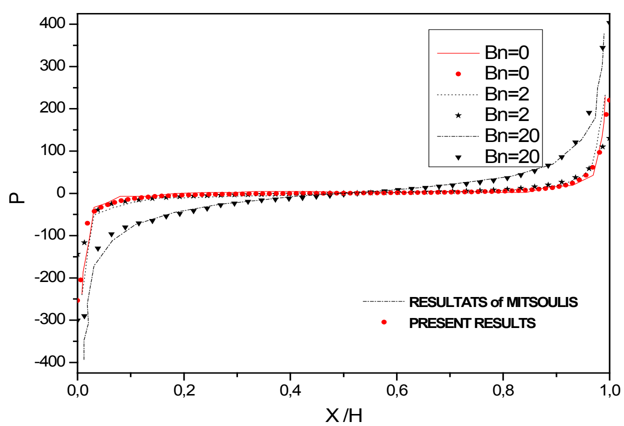

Figure 2: (b) Comparison of pressure distribution along the lid for different Bn numbers

4 Results and discussions

Fluid flow and heat transfer on mixed convection within a lid-driven square cavity filled by non-Newtonian fluid of Bingham model with heat source located at the bottom wall is investigated. A wide range of pertinent parameters are analyzed such as Reynolds number ranging from 1 to 100, R_i number from 1 to 20 and Bingham number from 0 to10.

4.1 Effects of Reynolds number

Fig. 3 reveals the effect of Reynolds number on the flow behavior through streamlines and isotherm contours for fixed Richardson number $R_i = 20$ and Bingham number Bn=2. For all Reynolds numbers the flow presents vertical mid-line axis symmetry, due to the geometry and boundary conditions, two equal magnitude counter-rotating cells are formed. Moreover, it is clear that the two thermal and dynamic forces are weak. For Reynolds number Re=1, which give rise to conduction mode as shown as a parabolic isotherms. The two cells formed in the cavity are due to the moving walls with low recirculation. It can be explained by the high velocity gradient near the moving walls and weak fluid motion in the center of the cavity. By increasing Reynolds number, the two forces are enhanced, that leads to the creation of a center thermal plume, while the two cells increased in shape and velocity recirculation. For high Reynolds number (and high Rayleigh number) the thermal plume became stronger and the thickness of the thermal boundary layer decreased, which indicates high temperature gradient near walls and high heat transfer. The two cells increased and became closer to each other with high velocity gradient in the center and low velocity gradient near the walls which indicates that the thermal force is dominant.

Re=1

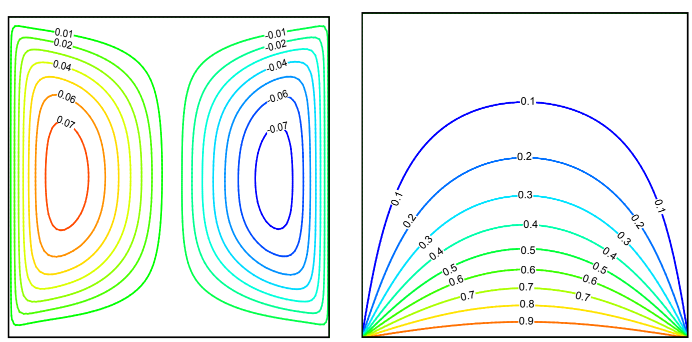

Re=10

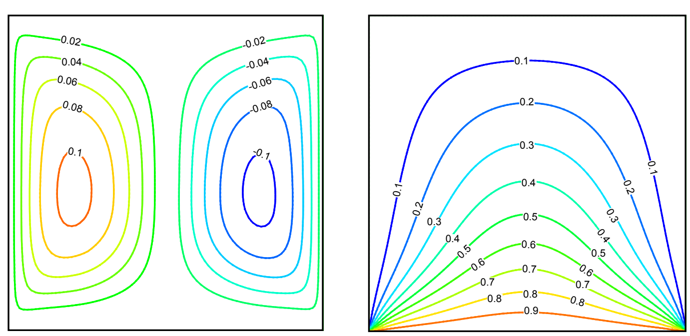

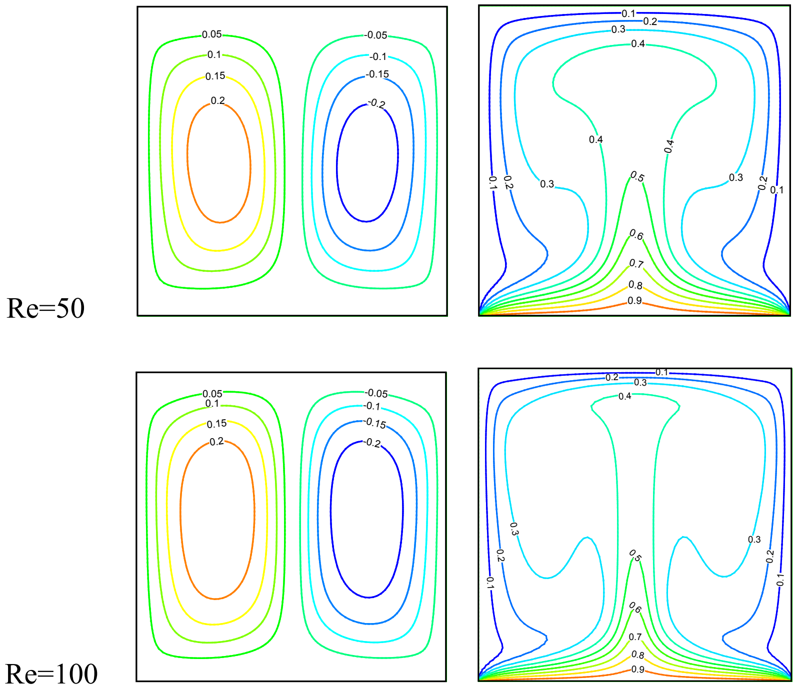

Figure 3: Flow patterns for Bingham fluid for different Reynolds numbers (R_i=20, B_n=2)

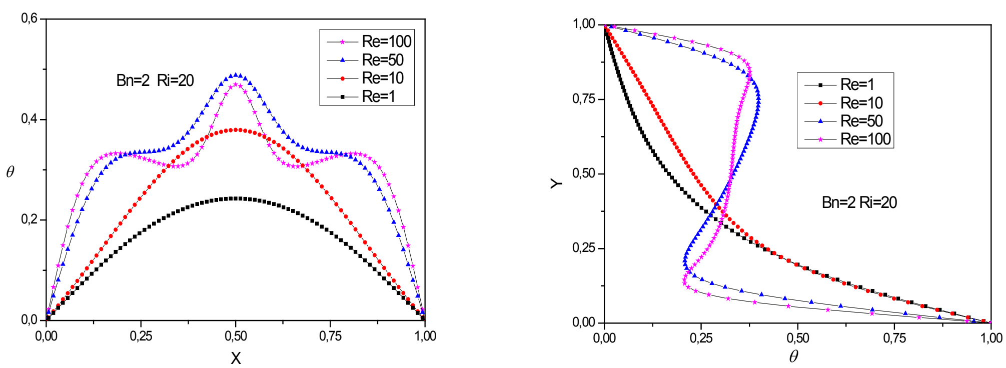

(a) (b)

Figure 4: Effect of Re number on non-dimensional temperature variations, for R_i=20, B_n=2, along: (a) the horizontal mid-plane (y=0.5), (b) the vertical mid-plane (x=0.5)

Fig. 4 displays the non-dimensional temperature variations along the horizontal mid-plane (y=0.5) and the vertical plane (x=0.25) for several Reynolds numbers. The temperature variation for low Reynolds number is given by parabolic isotherms due to the boundary conditions, and the conduction mode is dominant as mentioned in Fig. 3. In addition, the increase of Reynolds number causes the temperature distribution to be non-linear and the convective transport is enhanced for higher values of Reynolds number where the temperature gradient becomes important near the walls mainly in the bottom wall. A high temperature gradient was found in the two down corners of the cavity.

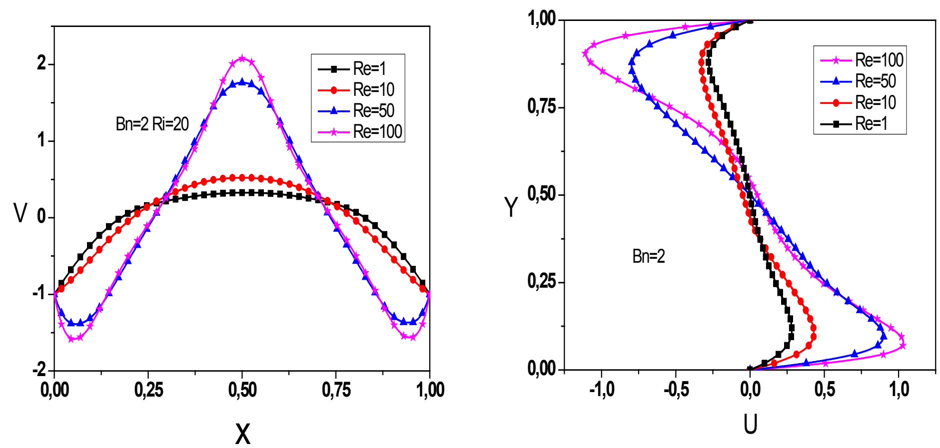

(a) (b)

Figure 5: Effect of Re numbers on the vertical velocity variations along: (a) the horizontal mid-plane (y=0.5) and (b) horizontal velocity along the vertical quarter-plane (x=0.25) R_i=20, B_n=2

Fig. 5 presents the vertical and the horizontal velocity variations for different Reynolds numbers. It indicates that the vertical velocity profiles are symmetric with respect to the mid-plane of the cavity, and its magnitude increased when increasing Reynolds number as might be exported based on the results in Fig. 4. On the other hand, the horizontal velocity profiles are not symmetric due to the change of the shape and the position of the cells recirculation, where they are pushed down towards the vertical walls for low Reynolds numbers, and they become stronger occupying the hole of the cavity with high velocity magnitude for high Reynolds numbers.

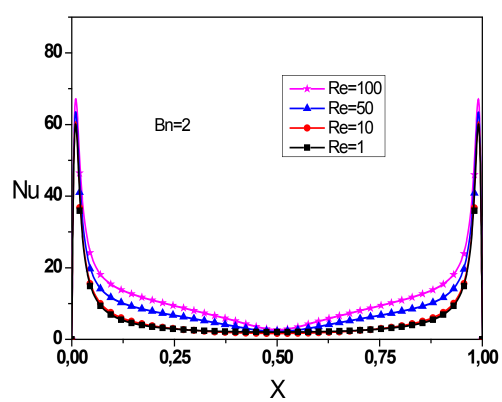

Figure 6: Effect of Re numbers on the Nusselt number variations along the heat source (bottom wall) (R_i=20, B_n=2)

Fig. 6 indicates the distribution of Nusselt number on the hot wall for different Reynolds numbers, shows that the Nusselt number augments gradually as the lid driven velocity augments. Whereas, the heat transfer is weak for low Reynolds number (Re=1) and the conduction mode governs the state. For high Reynolds number (Re=100), convection mode is dominant as presented in Fig. 3 which leads to increase the amount of heat transfer.

4.2 Effects of Richardson number

Fig. 7 presents flow patterns for different Richardson numbers at a fixed Reynolds number, Re=100. The fluid rises in the middle of the cavity in the form of a thermal plume due to buoyancy forces and descends near the cold vertical sides which move down. As a result two counter-rotating cells are formed within the cavity. The descent is enhanced by the lid movement. In addition, the isotherms are pushed toward to the bottom wall and the thermal boundary layer decreases indicating high temperature gradient and then high heat transfer due to the increase in the Richardson number. Whereas the centers of the rotating cells, which become larger, are pushed upward with a notable increase in the maximum of stream function.

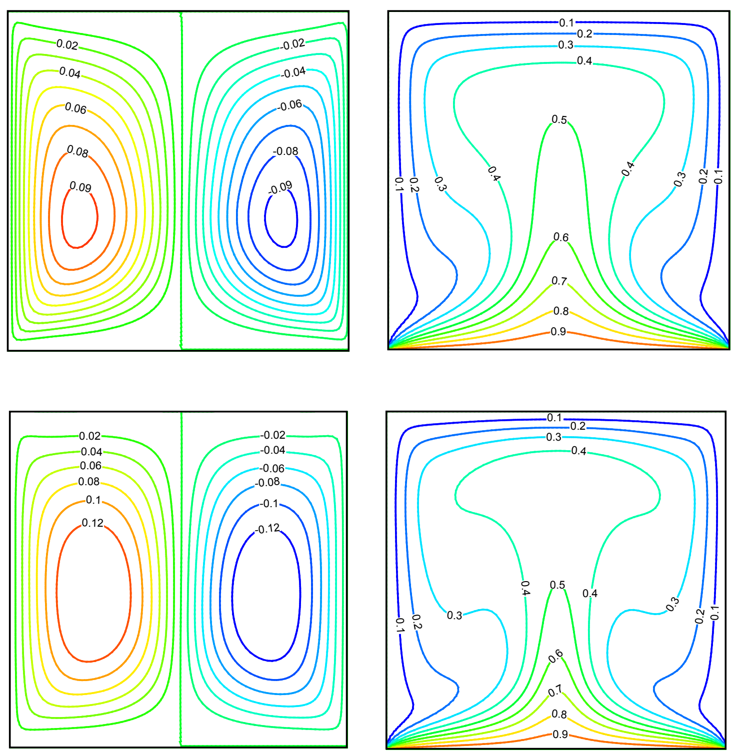

R_i=1

R_i=5

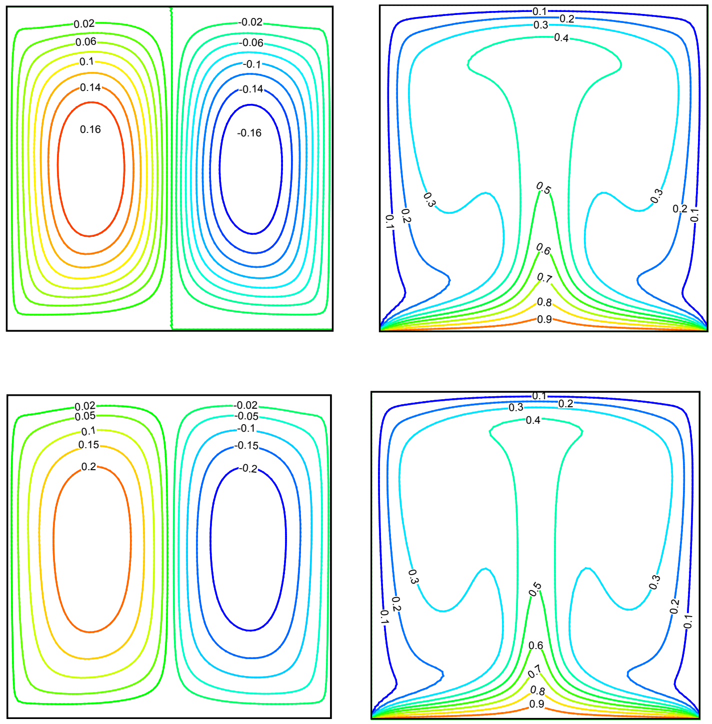

R_i=10

R_i=20

Figure 7: Effects of Richardson number on the Streamlines (left) and isotherms (right) contours for Bingham fluid (Re=100, B_n=2)

The temperature and the vertical velocity distributions for a Bingham fluid (at B_n=2) along the horizontal mid-plane for different Richardson numbers are shown in Fig. 8. The effect of buoyancy forces strengthen, relative to the viscous forces, when increasing Richardson number at fixed Bingham numbers. This leads to enhance the convection process due to stronger buoyancy-driven flow with higher vertical velocity magnitude. This effect is clearly evident from Fig. 8, which indicates that the vertical velocity magnitude increases indeed when increasing Richardson number where streamlines become closer showing high velocity gradient as presented in Fig. 7.

The distribution of non-dimensional temperature becomes increasingly non-linear with the strengthening of convective transport for high values of Richardson number. This strengthening is also mentioned in Fig. 7. From this figure, it is evident that isotherms become increasingly curved when Richardson number increases. This is due to a strong convective current within the enclosure, while isotherms are parallel to the wall due to the dominance of conduction heat transfer at low Richardson number.

Variation of the heat transfer rate quantified by the average Nusselt number, along the heated bottom wall for different Richardson numbers, is presented in Fig. 9. The results show that Nusselt number is enhanced relatively when Richardson number increases. However, for low Richardson number, the heat transfer is almost weak and the conduction mode governs the state. For high Richardson number (R_i=20), the heat transfer rate is increased due to convection mode which is dominant. This mechanism augments the amount of heat transfer. In addition, it can be observed that heat transfer given by Nusselt number is very high in the two corners at the bottom wall of the cavity, where the temperature gradient is very important as given by Fig. 3 and Fig. 7.

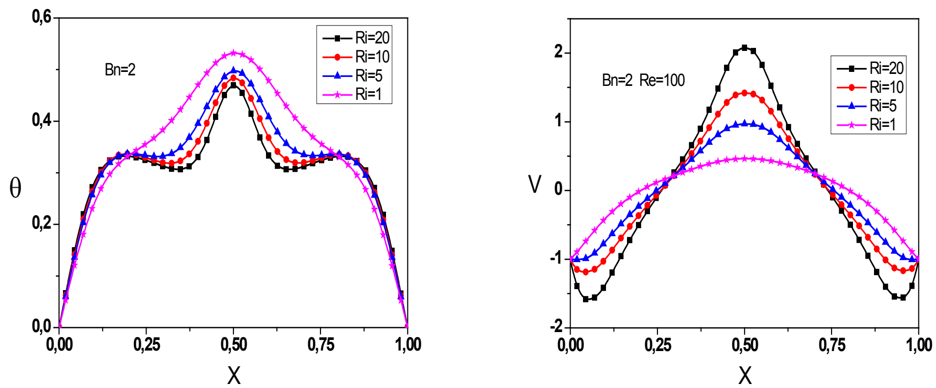

Figure 8: Variations of vertical velocity (right) and non-dimensional temperature (left) along the horizontal mid-plane for different R_i numbers at Re=100 and B_n=2

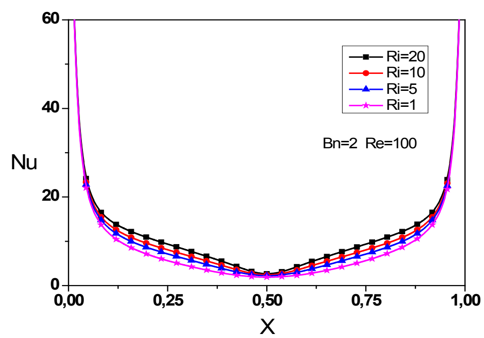

Figure 9: Effects of Richardson number on the Nusselt number variations along the bottom wall (Re=100, B_n=2)

4.3 Bingham and Prandtl numbers effects

The effects of Bingham number (B_n) on streamlines and isotherms are presented in Fig. 10. For low B_n number (B_n=0) which corresponds to the Newtonian fluid, two cells occupy the hole of the cavity with high fluid recirculation. While increasing Bingham number, the cells become weaker and localized in closer proximity to the moving lids as shown in Fig. 10. Moreover, isotherms show the thermal plume formation which is clear in the case of Newtonian fluid (B_n=0) and vanishing when Bingham number increases. It indicates that the Bingham fluid with high plasticity opposes the formation of the thermal plume where isotherms become parallel indicating that conduction mode is dominant.

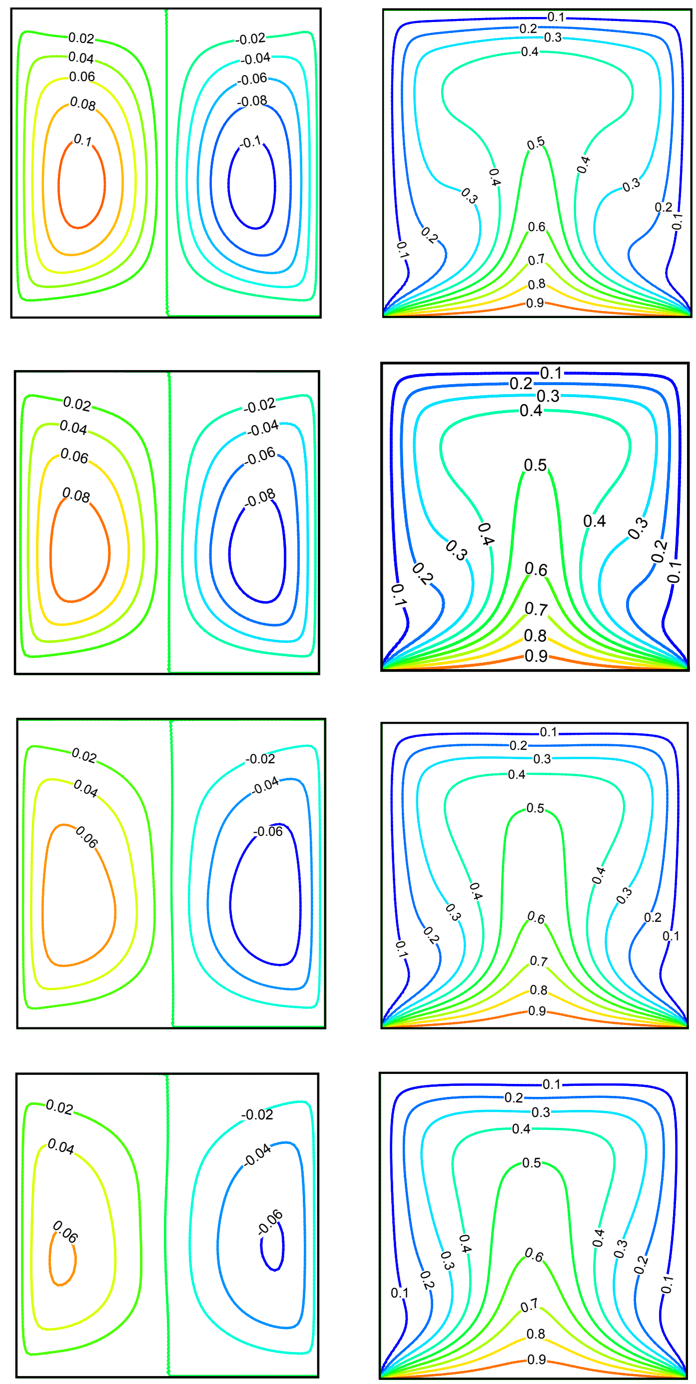

B_n=0

B_n= 2

B_n=5

B_n=10

Figure 10: Streamlines (left) and isotherms (right) contours for different Bingham numbers at Re=100 and R_i=1

Non-dimensional temperature and vertical velocity profiles along the horizontal mid-plane for different values of Bingham number and fixed values of Richardson number (R_i=1) and Reynolds number (Re=100) are shown in Fig. 11. The magnitude of vertical velocity and temperature variations along the mid-plane of the cavity decreased when increasing Bingham number, indicating weakness of thermal convective transport at the same nominal values of Richardson and Reynolds numbers. The additional flow resistance in Bingham fluids leads to the weakness flow in comparison with a Newtonian fluid (B_n=0), and this trend strengthens with increasing B_n. The weakness of convective transport can be confirmed from Fig. 10. Fig. 11 shows that the effects of convection fluid flow within the enclosure decreases when Bingham increases. So the fluid starts to behave as a solid-the fluid velocity decreases to such low values-whereas it is essentially stagnant in the center of the cavity for all practical purposes.

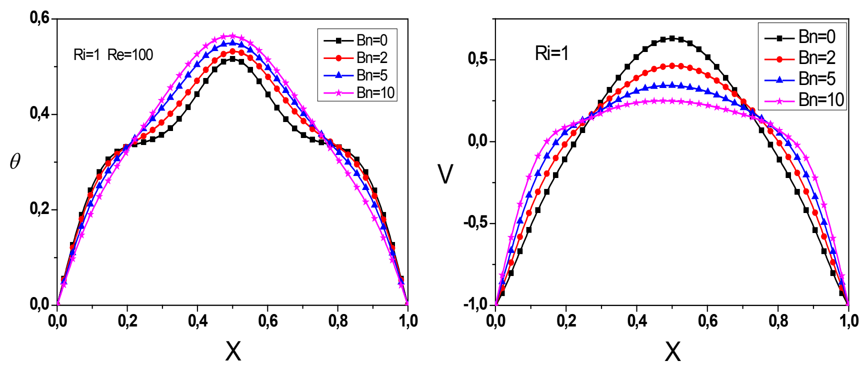

Figure 11: Non-dimensional temperature (left) and vertical velocity (right) variations along the horizontal mid-plane for different $B_n$numbers at Re=100 and R_i=1

Fig. 12 illustrates the variation of Nusselt number for different Bingham and Richardson numbers. As evident, heat transfer increases when increasing the buoyancy force for different fluid plasticity. Moreover, Nusselt number is high in the case of Newtonian fluid and low when increasing Bingham number where the fluid viscosity becomes higher which decreases the fluid strength recirculation. In addition, the thermal boundary layer thickness increases for high plasticity as presented in Fig. 10 showing low heat transfer compared to the Newtonian fluid.

The effect of Prandtl number on heat transfer for different Richardson numbers is depicted in Fig. 13. It shows that Nusselt number is strongly affected by the increase of Prandtl number where the momentum diffusivity is increased compared to thermal diffusivity. This is simply due to the progressive thinning of the thermal boundary layer indicating high temperature gradient and high heat transfer.

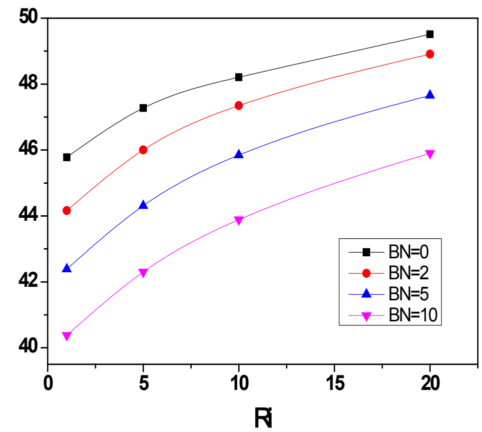

Figure 12: Influence of Richardson number, R_i and Bingham number, B_n on average Nusselt number

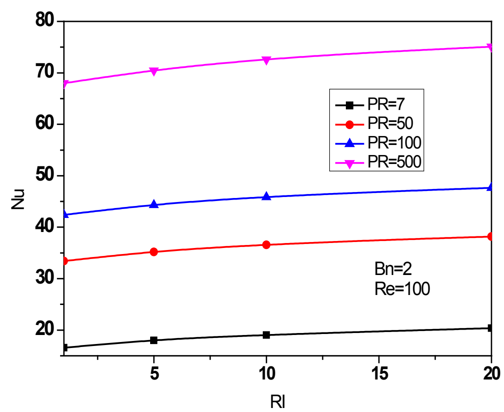

Figure 13: Influence of Richardson number, R_i and Prandtl number, Pr on average Nusselt number

4.4 Nusselt number correlation

The average Nusselt number increases when increasing Richardson, Reynolds and Prandtl numbers, while it drops at high Bingham numbers. The present numerical results are correlated using the following relationship summarizing the effects of the different parameters on heat transfer given by the Nusselt number:

$$\overline{\mathrm{Nu}} = \mathrm{m.}\ \mathrm{Ri}^{\mathrm{a}}.\mathrm{Re}^{\mathrm{b}}\,.\mathrm{Pr}^{\mathrm{c}}.\mathrm{Bn}^{\mathrm{d}} \tag{8}$$

where: m=1.63, a=0.067, b=0.3633, c=0.3318 and d=-0.055

Eq. (8) correlates the numerical results of Nusselt number for a given parameters: Richardson number ($1\leq R_i \leq 20$), Reynolds number ($1\leq Re\leq 100$), Prandtl number ($1\leq Pr\leq(500)$, and Bingham number ($2\leq B_n\leq 10$) with an average error of 5.4%.

Fig. 14 presents the correspondence plot between the numerical results of Nusselt number and the predictions of the Eq. (8).

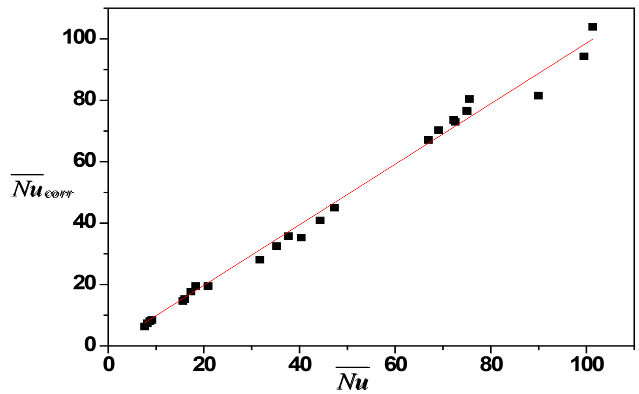

Figure 14: Parity plot between numerical results and predicted values using Eq. (8)

5 Conclusion

In this paper, we have carried out numerical simulation of mixed convection in a square cavity with two moving walls. The cavity was heated from the bottom wall and filled by Non-Newtonian fluid of Bingham model. The objective of this investigation was to study the Richardson and Reynolds numbers effects and the effect of the yield stress on fluid flow and heat transfer. Plots of streamlines and isotherms, and velocity profiles and Nusselt number are presented and discussed.

The results obtained show that forced convection is increased by increasing Reynolds number, which enhances the heat transfer. Furthermore, increasing Richardson number leads to enhance heat transfer, while high Bingham numbers weakening the fluid flow and decrease heat transfer. It is noted that for high yield stress, the fluid behaves like a solid and conduction mode is dominant.

References

Abu-Nada, E.; Chamkha, A. J. (2014): Mixed convection flow of a nanofluid in a lid-driven cavity with a wavy wall. *International Communications in Heat and Mass Transfer*, vol. 57, pp. 36-47.

Al-Amiri, A.; Khanafer, K.; Bull, J.; Pop, I. (2007): Effect of sinusoidal wavy bottom surface on mixed convection heat transfer in a lid-driven cavity. *International Journal of Heat and Mass Transfer*, vol. 50, no. 9-10, pp. 1771-1780.

Albensoeder, S.; Kuhlmann, H. C. (2002): Three-dimensional instability of two counter-rotating vortices in a rectangular cavity driven by parallel wall motion. *European Journal of Mechanics-B/Fluids*, vol. 21, no. 3, pp. 307-316.

Blohm, C. H.; Kuhlmann, H. C. (2002): The two-sided lid-driven cavity: experiments on stationary and time-dependent flows. *Journal of Fluid Mechanics*, vol. 450, pp. 67-95.

Cheng, M.; Hung, K. (2006): Vortex structure of steady flow in a rectangular cavity. *Computers & Fluids*, vol. 35, no. 10, pp. 1046-1062.

Cheng, T. (2011): Characteristics of mixed convection heat transfer in a lid-driven square cavity with various Richardson and Prandtl numbers. *International Journal of Thermal Sciences*, vol. 50, no. 2, pp. 197-205.

Karimipour, A.; Esfe, **M. H.; Safaei, M. R.; Semiromi**, **D. T.; Jafari, S. et al.** (2014): Mixed convection of copper-water nanofluid in a shallow inclined lid driven cavity using the lattice Boltzmann method. *Physica A: Statistical Mechanics and Its Applications*, vol. 402, pp. 150-168.

Khanafer, K. M.; Al-Amiri, A. M.; Pop, I. (2007): Numerical simulation of unsteady mixed convection in a driven cavity using an externally excited sliding lid. *European Journal of Mechanics-B/Fluids*, vol. 26, no. 5, pp. 669-687.

Khanafer, K. M.; Chamkha, A. J. (1999): Mixed convection flow in a lid-driven enclosure filled with a fluid-saturated porous medium. *International Journal of Heat and Mass Transfer*, vol. 42, no. 13, pp. 2465-2481.

Kuhlmann, H. C.; Albensoeder, S.; Blohm, C. (2001). Flow instabilities in the two-sided lid-driven cavity. *12th International Couette-Taylor Workshop*.

Kuhlmann, H. C.; Wanschura, M.; Rath, H. J. (1997): Flow in two-sided lid-driven cavities: non-uniqueness, instabilities, and cellular structures. *Journal of Fluid Mechanics*, vol. 336, pp. 267-299.

Mahapatra, S. K.; Nanda, P.; Sarkar, A. (2006): Interaction of mixed convection in two-sided lid driven differentially heated square enclosure with radiation in presence of participating medium. *Heat and Mass Transfer*, vol. 42, no. 8, pp. 739-757.

Mitsoulis, E.; Zisis, T. (2001): Flow of Bingham plastics in a lid-driven square cavity. *Journal of Non-Newtonian Fluid Mechanics*, vol. 101, no. 1-3, pp. 173-180.

Mojumder, S.; Sourav, S. A. H. A.; Sumon, S. A. H. A.; Mamun, M. A. H. (2015): Combined effect of Reynolds and Grashof numbers on mixed convection in a lid-driven T-shaped cavity filled with water-Al_2O_3 nanofluid. *Journal of Hydrodynamics*, vol. 27, no. 5, pp. 782-794.

Muthtamilselvan, M.; Doh, D. H. (2014): Mixed convection of heat generating nanofluid in a lid-driven cavity with uniform and non-uniform heating of bottom wall. *Applied Mathematical Modelling*, vol. 38, no. 13, pp. 3164-3174.

Nalluri, S. V.; Patel, S. A.; Chhabra, R. P. (2015): Mixed convection from a hemisphere in Bingham plastic fluids. *International Journal of Heat and Mass Transfer*, vol. 84, pp. 304-318.

Ouertatani, N.; Cheikh, N. B.; Beya, B. B.; Lili, T.; Campo, A. (2009): Mixed convection in a double lid-driven cubic cavity, *International Journal of Thermal Sciences*, vol. 48, no. 7, pp. 1265-1272.

Oztop, H. F.; Dagtekin, I. (2004): Mixed convection in two-sided lid-driven differentially heated square cavity. *International Journal of Heat and Mass Transfer*, vol. 47, no. 8-9, pp. 1761-1769.

Papanastasiou, T. C. (1987): Flows of materials with yield. *Journal of Rheology*, vol. 31, no. 5, pp. 385-404.

Patankar, S. (1980). *Numerical Heat Transfer and Fluid Flow*. CRC Press.

Shah, P.; Rovagnati, B.; Mashayek, F.; Jacobs, G. B. (2007): Subsonic compressible flow in two-sided lid-driven cavity. Part I: equal walls temperatures. *International Journal of Heat and Mass Transfer*, vol. 50, no. 21-22, pp. 4206-4218.

Sharif, M. A. R. (2007): Laminar mixed convection in shallow inclined driven cavities with hot moving lid on top and cooled from bottom. *Applied Thermal Engineering*, vol. 27, no. 5-6, pp. 1036-1042.

Sivakumar, V.; Sivasankaran, S.; Prakash, P.; Lee, J. (2010): Effect of heating location and size on mixed convection in lid-driven cavities. *Computers & Mathematics with Applications*, vol. 59, no. 9, pp. 3053-3065.

Turan, O.; Chakraborty, N.; Poole, R. J. (2010): Laminar natural convection of Bingham fluids in a square enclosure with differentially heated side walls. *Journal of Non-Newtonian Fluid Mechanics*, vol. 165, no. 15-16, pp. 901-913.

Turan, O.; Chakraborty, N.; Poole, R. J. (2012): Laminar Rayleigh-Bénard convection of yield stress fluids in a square enclosure. *Journal of Non-Newtonian Fluid Mechanics*, vol. 171, pp. 83-96.

Turan, O.; Poole, R. J.; Chakraborty, N. (2012): Boundary condition effects on natural convection of Bingham fluids in a square enclosure with differentially heated horizontal walls. *Computational Thermal Sciences: An International Journal*, vol. 4, no. 1.

Turan, O.; Sachdeva, A.; Poole, R. J.; Chakraborty, N. (2011): Laminar natural convection of Bingham fluids in a square enclosure with vertical walls subjected to constant heat flux. *Numerical Heat Transfer, Part A: Applications*, vol. 60, no. 5, pp. 381-409.

Waheed, M. A. (2009): Mixed convective heat transfer in rectangular enclosures driven by a continuously moving horizontal plate. *International Journal of Heat and Mass Transfer*, vol. 52, no. 21-22, pp. 5055-5063.

Yigit, S.; Poole, R. J.; Chakraborty, N. (2015): Effects of aspect ratio on natural convection of Bingham fluids in rectangular enclosures with differentially heated horizontal walls heated from below. *International Journal of Heat and Mass Transfer*, vol. 80, pp. 727-736.

Zhang, J.; Vola, D.; Frigaard, I. A. (2006): Yield stress effects on Rayleigh-Bénard convection. *Journal of Fluid Mechanics*, vol. 566, pp. 389-419.